1  Stability assessment of organic sulfur and organosulfate compounds in filter

2  samples for quantification by Fourier Transform-Infrared Spectroscopy

3  Marife B. Anunciado[1], Miranda De Boskey[2], Laura Haines[2], Katarina Lindskog[2],

4  Tracy Dombek[2], Satoshi Takahama[3], Ann M. Dillner[1]

6  [1]Air Quality Research Center, University of California Davis, Davis, California,

7  United States

8  [2]Research Triangle Institute, Research Triangle Park, North Carolina, United States

9  [3]Ecole Polytechnique Fédérale de Lausanne (EPFL), Switzerland

11  Corresponding author:

12  Ann M. Dillner

13  Air Quality Research Center, University of California, Davis

14  1560 Drew Ave., Davis, California, 95618, USA

15  Email: amdillner@ucdavis.edu

**Abstract**

18    Organic sulfur and sulfate compounds, tracers for sources and atmospheric processes, are not

19    currently measured in national monitoring networks such as the Interagency Monitoring of

20    Protected Visual Environments (IMPROVE). The goal of this paper is to begin to assess the

21    stability of organic sulfur and sulfate containing compounds on polytetrafluoroethylene (PTFE)

22    filters and the suitability of Fourier-transform infrared (FT-IR) spectroscopy to measure these

23    compounds. Stability assessment is needed because PTFE samples collected by IMPROVE are

24    typically stored 6-9 months prior to analysis. For this study, two organosulfur compounds,

25    methanesulfonic acid (MSA) and hydroxymethanesulfonate ion (HMS), and two organosulfate

26    compounds, methyl sulfate (MS) and 2-methyltetrol sulfate (2-MTS), are collected individually

27    on PTFE filters. Gravimetric mass measurements is used to assess mass stability over time. FT-

28    IR spectra are evaluated to assess the capability of measuring the compound from PTFE filters by

29    assessing the compound stability or chemical changes over time. Ion chromatography (IC) and

30    Inductively Coupled Plasma Optical Emission Spectroscopy (ICP-OES) are used as an additional

31    tool to assess stability or chemical changes over time. MS has the highest potential to be measured

32    by FT-IR in IMPROVE samples. For MS, a simple organosulfate, the mass changes are within

33    measurement uncertainty and FT-IR spectra indicate no compositional change over a 4-month

34    period, suggesting MS can be measured using FT-IR. IC and ICP-OES support the conclusion

35    that MS is stable on the filter. However, for 2-MTS, the other organosulfate measured in this study,

36    spectral changes after a month on the filter suggests it decomposes into other organosulfates or an

37    inorganic sulfate. MSA in IMPROVE samples can be measured, but only as a lower bound, due

38    to volatility off of the filter as indicated by FT-IR and gravimetry. FT-IR and IC both show that

39    MSA is not chemically changing over the course of the study. Measurements by all methods

40 indicate HMS is unstable on PTFE filter and IC and FT-IR indicate that it likely converts to

41 inorganic sulfate. Future work includes the evaluation of these compounds in as ambient aerosol

42 sample matrix to determine any differences in stability and identify interferences that could limit

43 quantification.

# 1. Introduction

44
45

46 Organic sulfur compounds exist in particulate form in the atmosphere and can be the result of

47 natural processes (e.g. marine sulfur, volcanic emissions) (Aneja and Cooper, 1989; Bates et al.,

48 1992) or activities of anthropogenic sources (e.g. combustion, sulfur-rich wastewaters, smelting)

49 (Grübler, 1998; Smith et al., 2011). Organic sulfur compounds can be categorized as

50 organosulfur compounds such as sulfones ($RSO_2$) and sulfonic acids ($RSO_3^-$) having C-S bonds,

51 while organosulfates ($ROSO_3^-$) have a C-O-S bond in the structure (Song et al., 2019). Two

52 sulfonic acid compounds, methanesulfonic acid (MSA), a tracer for marine aerosol, and

53 hydroxymethanesulfonate ion (HMS), measured in high haze conditions, along with two

54 organosulfates compounds, methyl sulfate (MS) and 2-methyltetrol sulfate (2-MTS) were

55 selected for evaluation.

56     Methanesulfonic acid forms from photochemical oxidation of dimethyl sulfide (DMS)

57 (Kwong et al., 2018b; von Glasow and Crutzen, 2004). DMS is a naturally occurring sulfur

58 species produced by marine algae or phytoplankton and is an important precursor of sulfur

59 dioxide, non-sea salt inorganic sulfate and organosulfur compounds, including MSA (Barnes et

60 al., 1994; Hoffmann et al., 2016). This makes MSA a tracer for marine aerosol (Allen et al.,

61 1997; Becagli et al., 2013; Saltzman et al., 1986). Ion chromatography (IC) has been used to

62 measure MSA in ambient aerosol collected on PTFE filters (Amore et al., 2022) and nucleopore

63 filters (Allen et al., 2002). MSA has also been measured in water soluble fractions of ambient

64 aerosol using proton nuclear magnetic resonance (HNMR) (Decesari et al., 2000). Fourier-

65 transform infrared spectroscopy (FT-IR) has been used to characterize liquid and solid MSA in

66 the laboratory studies (Chackalackal and Stafford, 1966; Lee et al., 2019; Zhong and Parker,

67 2018) as has Raman spectroscopy (Zhong and Parker, 2018), but to the best of our knowledge,

68    neither FT-IR or Raman spectroscopy have been used to measure MSA in complex mixtures like

69    ambient aerosol samples.

70        Hydroxymethanesulfonate (HMS), formed by sulfite and formaldehyde in aqueous phase,

71    is a strong acid that is stable at low pH (Seinfeld and Pandis, 2016) and is a tracer for aqueous

72    processes (Chen et al., 2022).  During severe winter haze in the North China Plain, HMS was

73    measured using real-time single particle mass spectrum instruments and filter-based IC methods

74    during periods of high $SO_2$ and HCHO concentrations and low oxidant concentrations in

75    particles with high liquid water content (Ma et al., 2020).  Very high concentrations of HMS

76    have been measured in Fairbanks, Alaska during pollution events in a cold, dark and humid

77    environment (Campbell et al., 2022). In the Interagency Monitoring of Protected Visual

78    Environments (IMPROVE) Network, there is evidence of an ubiquitous presence of HMS in ion

79    chromatograms of samples collected at 150 sites in the United States (Moch et al., 2020).

80        However, HMS can be challenging to measure (Moch et al., 2018).  Single particle mass

81    spectrometry techniques have identified m/z 111 as characteristic for HMS (Chapman et al.,

82    1990; Lee et al., 2003; Song et al., 2019).  However, methyl sulfate and other organic sulfur

83    compounds have the same characteristic m/z which makes quantifying HMS using mass

84    spectrometry challenging (Dovrou et al., 2019; Lee et al., 2003). High-resolution aerosol mass

85    spectrometry (HR-AMS) has been used to measure HMS and organosulfates, however the

86    majority of compounds  mostly fragment into inorganic sulfate and a non-sulfur containing

87    organic fraction, leading to an underestimation of HMS and overestimation of inorganic sulfate

88    (Dovrou et al., 2019; Song et al., 2019).  HMS has been measured in field and laboratory studies

89    by IC (Campbell et al., 2022; Dovrou et al., 2019), however notable challenges have been

90    documented. HMS and sulfate are not fully resolved in all IC methods (Campbell et al., 2022)

91    leading to poor resolution that can introduce error into the results for both HMS and sulfate

92    (Dovrou et al., 2019; Ma et al., 2020). In IC methods where HMS and sulfate are well resolved,

93    HMS and sulfite may be unresolved and co-elute with bisulfite  (Moch et al., 2018; Wei et al.,

94    2020). Additionally, HMS may degrade to sulfite and formaldehyde at the high-pH eluent used

95    in IC (Moch et al., 2020). Degradation of both HMS and sulfite may occur in aqueous solutions

96    prior to analysis or in the column during analysis and it's suspected that some of the sulfite

97    oxidizes to sulfate in solution or in the column (Moch et al., 2020).  The formation of HMS in

98    the atmosphere occurs at moderate pH and pH differences, between the filter and atmospheric

99    condition (e.g. cloud, fog, pH), can contribute to HMS sample mass loss off the filter leading to

100   an underestimation of HMS (Moch et al., 2020). With proper columns and eluent composition,

101   IC has been shown to separate HMS and sulfate peaks with only a small underestimation of

102   HMS due to sulfate conversion (Campbell et al., 2022; Dovrou et al., 2019).  At least one

103   laboratory study (published in Japanese) has characterized HMS by FT-IR (Sato et al., 1984) but

104   FT-IR has not been used to measure HMS in ambient aerosol samples to the best of our

105   knowledge.

106   Organosulfates are the most abundant form of organic sulfur compounds in atmospheric particles

107   (Frossard et al., 2011; Hawkins et al., 2010; Hettiyadura et al., 2015; Olson et al., 2011; Stone et

108   al., 2012).  Organosulfates are secondary organic aerosols (SOA) from oxidation of mostly

109   biogenic, but also some anthropogenic volatile organic compounds, in the presence of acidic

110   sulfate (Hettiyadura et al., 2015; Stone et al., 2012; Wang et al., 2021) and have been suggested

111   to be tracers for SOA (Chen et al., 2021; Wang et al., 2021). Organosulfates have been measured

112   in ambient aerosol globally including at four sites in Asia where on average they contribute <1%

113   of $PM_{2.5}$, 2.3% of organic carbon and 3.8% of total sulfate (Stone et al., 2012). In Arctic haze

114  aerosols in the spring, organosulfates contributed to 13% of organic matter (OM) (Hansen et al.,

115  2014) and contributed to OM at varying levels across the US, with higher levels in summer

116  (Chen et al., 2021).  Most studies have used a liquid chromatography method coupled to a mass

117  spectrometer (LC-MS) for measuring organosulfates (Hettiyadura et al., 2015; Wang et al.,

118  2021). FT-IR has been used to measure total organosulfate functional groups (Hawkins et al.,

119  2010) and Raman (Bondy et al., 2018; Lloyd and Dodgson, 1961) and FT-IR (Lloyd et al., 1961)

120  have been utilized to characterize organosulfates in laboratory studies.  FT-IR has been used to

121  measure the organosulfate functional group using peak fitting and showed that the organosulfate

122  functional group contributes up to 10% of organosulfate in the arctic region, when inorganic

123  sulfate concentrations are considered high (Frossard et al., 2011), and 4-8% of OM in the Pacific

124  marine boundary layer, during periods of high organic and sulfate concentrations (Hawkins et al.,

125  2010). While other studies showed little to no organosulfates, likely due to low sulfate

126  concentrations in Mexico City (Liu et al., 2009) and Bakersfield, CA (Liu et al., 2012).

127  Methyl sulfate is the smallest organosulfate (Kwong et al., 2018a) and measured mostly in trace

128  amounts (Hettiyadura et al., 2017, 2015; Wang et al., 2021). However, it is commercially

129  available and therefore useful for laboratory studies.  2-Methyltetrol sulfates are tracers for

130  secondary organic aerosols (SOA) formation in atmospheric particles derived from isoprene

131  (Chen et al., 2020; Surratt et al., 2010) and one of the most abundant organosulfates measured in

132  ambient aerosol. In the eastern US, 2-MTS accounts for the highest percentage summertime

133  particulate organosulfate (11%) (Chen et al., 2021). In Centreville, AL, 2-MTS accounts for

134  more than half of organosulfates during summer of 2013 (Hettiyadura et al., 2017). In Shanghai,

135  China (summer of 2015-2016, 2018-2019), 2-MTS was the most abundant organosulfate (31%)

136  of 29 organosulfates (Wang et al., 2021).

137    The IMPROVE network is a rural particulate matter monitoring network with ~165 sites

138    across the United States (http://vista.cira.colostate.edu/improve/).  Polytetrafluoroethylene

139    (PTFE), nylon and quartz filters are used to collect PM$_{2.5}$ every one in three days, have a field

140    latency period of up to 7 days and are analyzed by multiple analytical techniques.  PTFE filters

141    are stored at room temperature and analyzed between 3 and 12 months after collection (typically

142    6 to 9 months) for PM mass, elements and filter-based light absorption.  Recently, FT-IR

143    analysis, a non-destructive method, has been performed on IMPROVE samples to reproduce

144    routinely measured compositional data (Debus et al., 2022) and measure the functional group

145    composition of the organic fraction (Ruthenburg et al., 2014). FT-IR analysis has also been

146    conducted on other networks and in chamber and field studies to measure organic functional

147    groups (Boris et al., 2021, 2019; Laurent and Allen, 2004; Russell et al., 2011; Ruthenburg et al.,

148    2014; Yazdani et al., 2022). The extracts of nylon filters have been analyzed by ion

149    chromatography (IC) in the IMPROVE network for more than three decades to routinely

150    measure the inorganic ions, sulfate, nitrate, chloride and nitrite.

151    (http://vista.cira.colostate.edu/improve/wp-content/uploads/2020/02/1_Anion-Cation-Analysis-

152    by-Ion-Chromatography-SOP-revision-7.pdf).  Although not routinely measured in IMPROVE

153    samples, HMS has been identified in IMPROVE samples using IC (Moch et al., 2020).

154    Organosulfates and MSA have been previously identified in extracts of IMPROVE samples

155    (Chen et al., 2021) using  hydrophilic interaction liquid chromatography interfaced to

156    electrospray ionization high-resolution quadrupole time-of-flight mass spectrometry (HILIC-

157    ESI-HR-QTOFMS).

158    The goal of this paper is to assess the potential for using FT-IR analyses to measure

159    organic sulfur compounds collected on PTFE filters in the IMPROVE network.  Measuring

160   organic sulfur compounds on a continuous basis across the US would provide a rich data set to

161   evaluate their sources, concentration, seasonality and trends over time.  Four organic sulfur

162   compounds, two organosulfur compounds, methanesulfonic acid, hydroxymethanesulfonate, and

163   two organosulfates, methyl sulfate and 2-methyltetrol sulfate, are evaluated.  For these

164   compounds to be measurable in IMPROVE by FT-IR, there must be minimal losses or other

165   changes to the compound during the latency period between collection and analysis (3 – 12

166   months), and there must be minimal interferences in the spectra.  To achieve this goal, each

167   compound was dissolved in solution, aerosolized and collected on PTFE filters.  Collected

168   samples were weighed and analyzed by FT-IR every few days for two months or more.

169   Characterization of the FT-IR spectra as well as changes (or lack therefore of) in the mass

170   loading and spectra over time indicate the potential for the compounds to be measured by FT-IR

171   in IMPROVE samples.  Filter samples, extracted for IC analysis at different time points, indicate

172   stability or chemical changes in the compound on the filter, assists with interpreting gravimetric

173   mass and FT-IR spectra changes.

## 2.  Materials and Methods

175   Two organic sulfur (C-S) compounds, MSA and HMS, and two organosulfates (C-O-S), MS and

176   2-MTS, were selected.  The four compounds were selected for this study based on following

177   three criteria. The compound 1.) has been measured in atmospheric particulate matter and is of

178   interest to the atmospheric science community, 2.) is water soluble so it can be put into solution

179   for atomization, and 3.) is available in high purity form to minimize uncertainty in mass

180   measurement.  Filter samples of the organic sulfur compounds were prepared for FT-IR,

181   gravimetry, IC and ICP-OES analyses by aerosolizing each compound individually and

182   collecting it on PTFE filters (Pall Corporation, 25 mm diameter).  One set of filters was

183 generated for analysis by gravimetry and FT-IR at UC Davis and another set (or sets depending

184 on what was being evaluated) of filters were generated for analysis by IC and ICP-OES at

185 Research Triangle Institute (RTI) following gravimetric analysis at UC Davis. Analyses of

186 these laboratory filter samples were performed to characterize the compound within infrared

187 spectra and to determine the stability of these compounds over time.

188 2.1 Preparation of laboratory filter samples

189     Three commercially available standards were used for this study: HMS sodium salt

190 (>97% purity, TCI America), MSA (100% purity, Sigma Aldrich) and MS sodium salt (100 %

191 purity, Sigma Aldrich). 2-methytetrol sulfate ammonium salt was synthesized following a

192 published method (Cui et al., 2018). Each compound was collected on PTFE filters by first

193 preparing an aqueous solution with a concentration of 0.005 M. For HMS, the solution was

194 acidified with hydrochloric acid (HCl) prior to aerosolization to obtain samples with

195 atmospherically relevant pH (pH 2), as pH plays a role in the stability of HMS. 2 µL of 1 M HCl

196 was added to HMS solution to obtain the final volume of 200 mL for aerosolization. Aerosols

197 were generated using an atomizer (Kamruzzaman et al., 2018; Ruthenburg et al., 2014) and dried

198 with a diffusion dryer (Model 3074B Filtered Air Supply, TSI Inc., St. Paul, MN). Dry particles

199 were collected on PTFE filters (Pall Corporation, 25 mm diameter) using an IMPROVE sampler

200 with varying collection times (40 to 720 s) at a flow rate of 22.4 L/min.

201 2.1.1  Gravimetric mass determination

202     Filter mass, before and after particle collection, was measured using an ultra-

203 microbalance (XP2U, Mettler-Toledo, Columbus, OH) with 0.1 µg sensitivity. Ionizing

204 cartridges (Staticmaster® Model 2U500, Grand Island NY) housed on a flexible stand

205 (Staticmaster® Model BF2-1000, Grand Island NY) and Haug strip (Mettler Toledo 11140160,

206    Columbus, OH) were utilized to help eliminate static for more stable, accurate measurements.

207    Prior to particle collection, the mass of a filter was determined by the average of 5 mass

208    measurements taken on separate days. Only filters that weighed within measurements precision

209    for 25 mm filters ($\pm$ 6 µg) for the 5 measurements were used. After particle collection, filters

210    were allowed to achieve equilibrium at room temperature for 24-hrs. Filters were weighed for

211    three consecutive days in the 1st week, twice per week during 2nd – 4th weeks and once in the

212    weeks thereafter. The experiment was ended when the weights were stable for a month or more.

213    2.2 Infrared spectra collection and processing

214    FT-IR spectra of the filter samples of each compound were collected using a Tensor II FT-IR

215    spectrometer (Bruker Optics, Billerica, MA) with a liquid nitrogen cooled cadmium telluride

216    (MCT) detector over the spectral range of 4 000–400 cm$^{-1}$. Filters were placed in a house-built

217    sample chamber that is purged of water and $CO_2$ (PureGas) for 4 min before spectra acquisition

218    (Debus et al., 2019). Measurements were made using 512 scans for each filter at 4 cm$^{-1}$

219    resolution and ratioed to the most recent (less than 1 h) background spectrum to obtain

220    absorbance spectra using OPUS software (Bruker Optics, Billerica, MA, (Debus et al., 2019)).

221        To better visualize functional groups in the organosulfur compounds, spectra were

222    baseline corrected from 1500 cm$^{-1}$ to 500 cm$^{-1}$, using blank correction and smoothing spline

223    fitting (Kuzmiakova et al., 2016). The spectral region from 4000 cm$^{-1}$ to 1500 cm$^{-1}$ were

224    baselined using an automated version of the Kuzmiakova et al., 2016 smoothing spline process in

225    AirSpec (Reggente et al., 2019). Regions with large PTFE absorption (1300-1100 cm$^{-1}$, 700-600

226    cm$^{-1}$ and 500-420 cm$^{-1}$) were grayed out in spectra plots and are not considered for peak

227    identification. A baseline corrected spectrum of each compound is shown in supplemental

228    material Figure S1.

229    2.3  IC and ICP-OES sample analysis

230    PTFE filters of each organic sulfur and organosulfate sulfur compound were generated and

231    weighed at UC Davis prior to shipping the filters cold overnight to RTI for IC and ICP-OES

232    analysis. On the day the filters arrived at RTI, the filters were extracted in 50 ml of deionized

233    water ($18M\Omega$ cm$^{-1}$, Millipore Milli-Q Darmstadt, Germany), sonicated for 30 minutes in an ice

234    bath and placed on a shaker table in a cold room for 8 hours prior to analysis.  The PTFE filter

235    remained in the extraction vial for the duration of these experiments.

236    IC analysis was performed on Dionex Thermo Scientific ICS-3000 and ICS-6000 (Sunnyvale,

237    CA) instruments using suppression and conductivity detection. For MSA, extracts were analyzed

238    using the AS19 analytical and AG19 guard columns (anion hydroxide method) for initial

239    extraction efficiency tests and AS28 analytical and AG28 guard columns (hydroxide method) for

240    the subsequent analyses to evaluate changes over time.  HMS and MS extracts were analyzed

241    with AS12A analytical and AG12A guard columns (anion carbonate method), which has been

242    shown to provide sufficient separation of HMS and sulfate, but not separation of sulfite/bisulfite

243    and HMS (Dovrou et al., 2019).   MS extracts were analyzed with AS12A analytical and AG12A

244    guard columns (anion carbonate method), the same method as HMS. An IC method for analyzing

245    2-MTS had not been developed and evaluated prior to this work.  Eluent concentrations and flow

246    rates were optimized for best separation of all ions of interest.

247    ICP-OES, used to measure total sulfur on the filter, was performed on a Thermo Scientific iCAP

248    7600 duo analyzer (Bremen, Germany). The ICP-OES was run in axial mode using a sprint valve

249    and data were collected at 180.731 nm. The ICP-OES system was calibrated using the sulfate

250    calibration standards and validated using the sulfate calibration verification solutions described

251    below.

252  IC and ICP-OES systems were calibrated with calibration standards prepared via serial dilutions

253  of single source stock standards using a primary source. A secondary source was used to prepare

254  calibration verification solutions to validate the instrument calibration for all compounds except

255  for 2-MTS, for which a second source standard was unavailable.

256       Primary and secondary sources of National Institute of Standards and Technology

257  (NIST)-traceable solutions were purchased and used to prepare calibration standards and

258  calibration verification solutions respectively, for sulfate analyses by both IC and ICP-OES.

259  When NIST-traceable solutions were unavailable, salts were used to prepare calibration

260  standards and calibration verification  solutions for MSA, HMS, and MS. Vendor information for

261  primary and secondary sources are provided in Table S2 in supplemental material.  Certified

262  American Chemical Society (ACS)-grade sodium carbonate ($Na_2CO_3$) obtained from Fisher

263  Scientific (Fairlawn, NJ) and sodium bicarbonate ($NaHCO_3$) obtained from EMD Sciences

264  (Gibbstown, NJ) were used to prepare IC eluent when using anion carbonate methods for

265  analyses. Potassium hydroxide eluent generator cartridges purchased from Thermo Scientific

266  were used for eluent preparation for analyses conducted with anion hydroxide methods.  NIST-

267  traceable, 1000 µg/mL stock solutions of yttrium (Y) and cesium (Cs) obtained from High Purity

268  Standards (Charleston, SC) were used to for internal standard and ionization suppression,

269  respectively for ICP-OES measurements.

## 3. Results and Discussion

270

271  **Methanesulfonic acid**

272       Gravimetry

273  Mass changes, measured by gravimetry, for four methanesulfonic acid filter samples with masses

274  ranging from 64 µg to 80 µg are shown in Figure 1. Mass decreases steadily during the first

275     month to approximately 50% of the initial mass.  During the second month of measurements, the

276     mass remains constant ($50 \pm 6\%$).
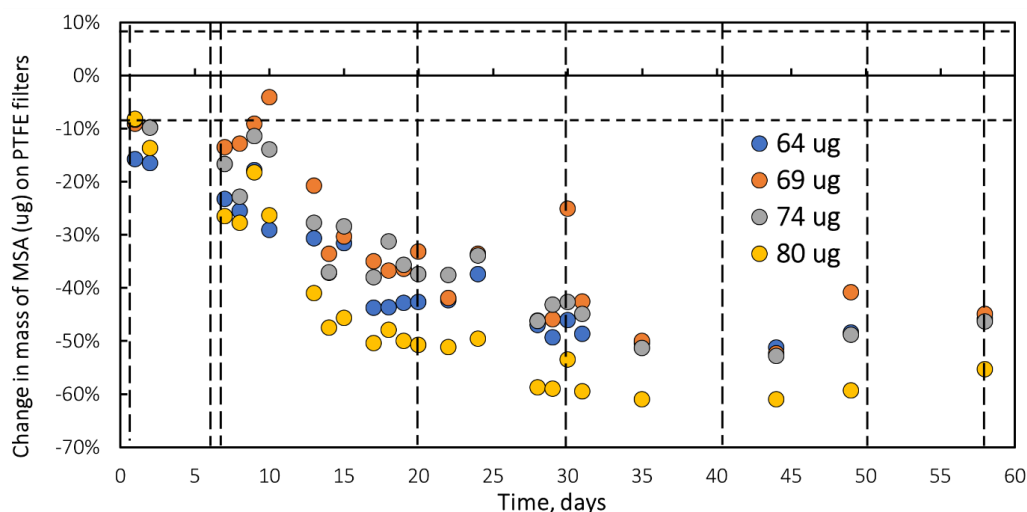
277

278     Figure 1. Change in mass of methanesulfonic acid (MSA) collected on PTFE filters over a 2-

279     month period under laboratory conditions (24 C˚C). Dotted vertical lines indicate FT-IR analysis.

280     Horizontal broken line indicates mass balance precision. Colors indicate initial masses of

281     samples.

282         FT-IR

283     Methanesulfonic acid ($CH_3SO_3H$) is composed of a methyl group attached to a sulfonic acid

284     [$S(=O)_2$─OH], via a C-S bond. Methanesulfonic acid aerosols collected on PTFE filters have

285     peaks associated with $CH_3$, $SO_3$, S-OH and C-S bonds (Figure 2).  Observed peaks (Figure 2)

286     can be ascribed to portions of the molecule based on previous FT-IR and Raman work

287     (Chackalackal and Stafford, 1966; Lee et al., 2019; Zhong and Parker, 2018).  The peaks at 1342

288     $cm^{-1}$ and 536 $cm^{-1}$ arise from S=O bonds in MSA and are shifted compared to inorganic peaks at

289     1130 $cm^{-1}$, 620 $cm^{-1}$ (Larkin, 2018) or organic sulfate $SO_4$ peaks at ~1380 $cm^{-1}$ (Larkin, 2018;

290    Lin-Vien et al., 1991). The peak at 895 cm$^{-1}$ is attributable to S─OH (Zhong and Parker, 2018)

291    and the peak at 766 cm$^{-1}$ is attributable to C-S (Lee et al., 2019). C-H peaks are observed at 3039

292    cm$^{-1}$, 2951 cm$^{-1}$, 1414 cm$^{-1}$ and 987 cm$^{-1}$ (Chackalackal and Stafford, 1966).  The broad peak at

293    3248 cm$^{-1}$ is suggested to be water as (Zeng et al., 2014) showed that this peak in MSA infrared

294    spectra increases with increasing RH.  These peaks, particularly strong peaks, were similar to

295    spectral absorbance of MSA from reference spectra (AIST: SDBS, 2022), and Table S1 in

296    Supplemental Materials compares the observed and reference peaks.
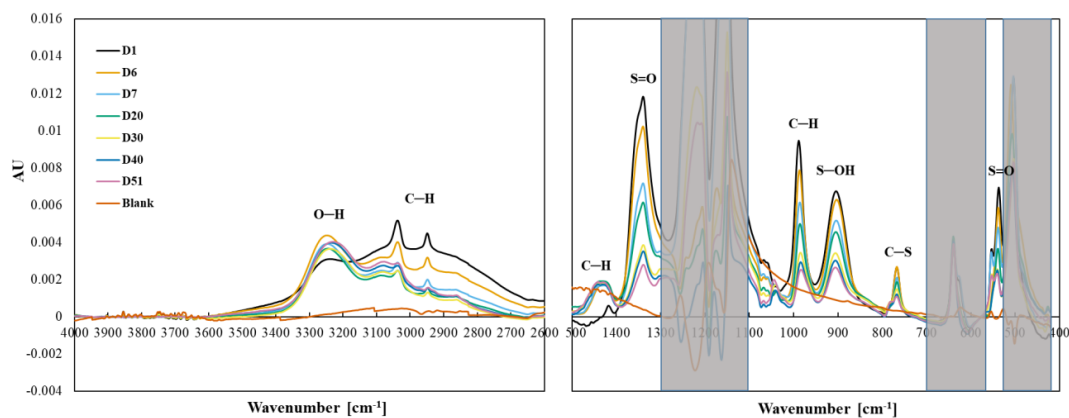
297

298    Figure 2. Changes in the spectra of MSA over a 2- month period, denoted by number of elapsed

299    days. The shaded area indicates the absorbance regions of PTFE filter.

300    The MSA infrared peaks of SO$_3$ (1342 cm$^{-1}$), C─H (987 cm$^{-1}$), S─OH (895 cm$^{-1}$), C-S (766 cm$^{-}$

301    $^1$), and S=O (536 cm$^{-1}$) decrease rapidly in the first 30 days, consistent with the decline in mass

302    during that time.  The spectra suggest that MSA is volatilizing off the filter, even though this is

303    inconsistent with the low vapor pressure of MSA (Knovel, 2014), 0.00022 mmHg at 20°C.  The

304    three spectra obtained on days 30, 41 and 51 show only small decreases which is mostly

305    consistent with the lack of mass changes during those days.

306    Not all peaks show consistent loss during the first month and little change during the second

307    month. The C-H peaks at 3039 cm$^{-1}$ and 2942 cm$^{-1}$ behave slightly differently, reaching stability

308    (with some minor random variability) earlier (day 20) than most other peaks. The weak peak at

309    1414 cm$^{-1}$ (ascribed to CH$_3$) increased and broadened to 1445 cm$^{-1}$ - 1400 cm$^{-1}$ after the initial

310    spectra was collected and remained fairly stable for the duration of the experiment. The peak at

311    3250 cm$^{-1}$, increased rapidly followed by fluctuations, and then varies somewhat but remained

312    fairly consistent for the duration of the experiment, not unlike the behavior of the 1414 cm$^{-1}$

313    peak.  One possible cause for these spectra changes in the spectra is water vapor condensing on

314    the particles after collection. MSA is hygroscopic and although it effloresces at about RH = 50%,

315    (Peng and Chan, 2001; Tang, 2020; Zeng et al., 2014), Zeng et al., 2014 shows that there is some

316    water associated with the particles below 50% RH, which is consistent with the FT-IR spectra

317    (Figure 3), particularly the 3248 cm$^{-1}$ peak.  If water is indeed the cause, the change in the 3248

318    cm$^{-1}$ peak can be explained by a very low RH in the particle generation and collection system

319    (lower initial peak) and a higher RH (RH = 30 $\pm$ 10%) in the lab (increase in peak).  The change

320    in the 1414 cm$^{-1}$ peak above 1400 cm$^{-1}$ behaves similarly, and can be associated with OH

321    suggesting uptake of water after the initial FT-IR spectra was collected.

322    Another possibility is that ammonia is absorbing onto the MSA. Ammonium absorbs in both the

323    3250 cm$^{-1}$ and 1500-1400 cm$^{-1}$ regions (Boer et al., 2007; Zawadowicz et al., 2015) and when

324    comparing  MSA spectra to ammonium sulfate spectra, they show very similar peak absorbance

325    and shapes in these two regions suggesting. This suggests that the cause of these peaks is

326    ammonium (Supplemental Material, Figure S2).

327    A third possible cause for these changes is that MSA may be fragmenting into formaldehyde

328    (CH$_2$O), that partitions into the gas phase, and sulfite (SO$_3$) (Kwong et al., 2018b).  However,

329    this would show a decrease in CHC-H peaks and a shift in the SOS=O peaks, neither of which

330    are observed in the spectra. The rapid decrease in peak height during the first month and then

331    little decrease or no trend during the second month, suggests that MSA is volatilizing off the

332    filter initially, but then has a slow decline, offset by increases in water or ammonium.

333        IC and ICP-OES

334    Twenty PTFE filters with MSA (14 µg – 32 µg; 60 µg – 144 µg) were shipped to RTI for

335    extraction and analysis by IC and ICP-OES. Each extract was analyzed by both IC and ICP-OES.

336    Recoveries of MSA from PTFE filters was $55 \pm 5\%$ for IC and $51 \pm 5\%$ for ICP-OES.

337    Calibration verification solution recoveries were $96 \pm 5\%$ for IC and $101 \pm 3\%$ for ICP-OES

338    analyses, suggesting that the lower recoveries from the PTFE filter are due to incomplete

339    extraction and/or losses occurring during shipment. To evaluate losses during shipping, six

340    samples were collected, weighed, and analyzed by FT-IR, shipped to RTI and then sent back to

341    UC Davis and analyzed with gravimetric and FT-IR analysis 9 days after initial measurements.

342    The mass loss ($19 \pm 7\%$) during this period was similar to mass loss for filters that remained in

343    the UC Davis laboratory for ~8 days ($22 \pm 6\%$). Spectral changes in shipped filters were similar

344    to changes in spectra that occurred during the first week for filters that remained at UC Davis.

345    To evaluate changes in mass and composition on PTFE filters over time, 6 filters (42 µg – 63 µg)

346    were shipped to RTI and extracted on days 0, 30, and 61. These filters had consistent recoveries

347    over time of $57 \pm 6\%$ for IC and $55 \pm 6\%$ for ICP-OES. The IC results indicate that MSA did

348    not change chemically during this time period, supporting the FT-IR spectral results. The mass

349    and spectral data indicate that the lower extraction efficiency was not due to loss of MSA off the

350    filter during shipping and suggest that the limitation is extraction efficiency. Despite low

351    extraction efficiencies and difference in behavior over time from FT-IR measurement, the FT-IR,

352    gravimetry and IC results suggest that a lower-bound of MSA can be measured on PTFE filters

353    in IMPROVE by FT-IR.

354    **Hydroxymethanesulfonate**

355        Gravimetry

356    Mass changes in three hydroxymethanesulfonate sodium salt (HOCH$_2$SO$_3$Na) filter samples with

357    mass loadings of ~62 µg per filter are shown (Figure 3). Mass decreases steadily for 1.3 months

358    to a maximum loss of 38% and then remains constant (38 $\pm$ 3%) for the rest of the experiment

359    (4.1 months).  Similar results were obtained for filters weighing approximately 30 µg/filter of

360    HMS.

361
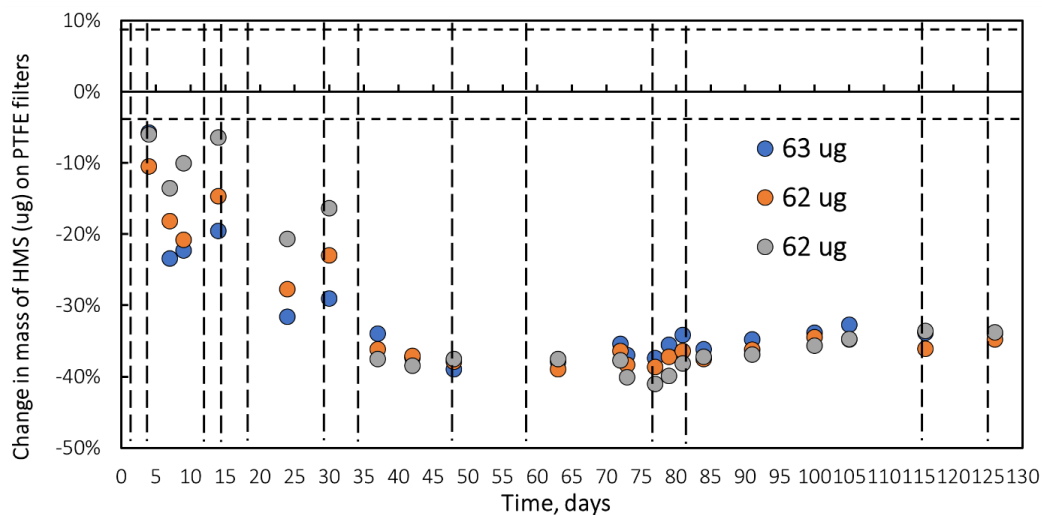
362

363    Figure 3. Mass behavior of hydroxymethanesulfonate (HMS) over 125 days under laboratory

364    conditions (~24°C).  Dotted vertical lines indicate FT-IR analysis. Horizontal broken line

365    indicates mass balance precision.

366

367        FT-IR

368   HMS (HOCH$_2$SO$_3$H) is a sulfonic acid compound with C-S bond, where the S bond is part of a

369   sulfonic acid group [S(=O)$_2$—OH],  and the carbon is attached to an –OH functional group,

370   similar to MSA except with the OH functional group attached to the carbon.  The chemical used

371   in our study has a sodium cation on the sulfonic acid group. HMS aerosol collected on  PTFE

372   filters have three infrared peaks (1094 cm$^{-1}$, 1041 cm$^-$and$^1$, 611 cm$^{-1}$) between 1500 and 500 cm$^{-1}$

373   , although the peak at 611 cm$^{-1}$ is obscured by PTFE absorption, and O-H and C-H peaks

374   between 4000 cm$^{-1}$ and 1500 cm$^{-1}$ (Figure 4).
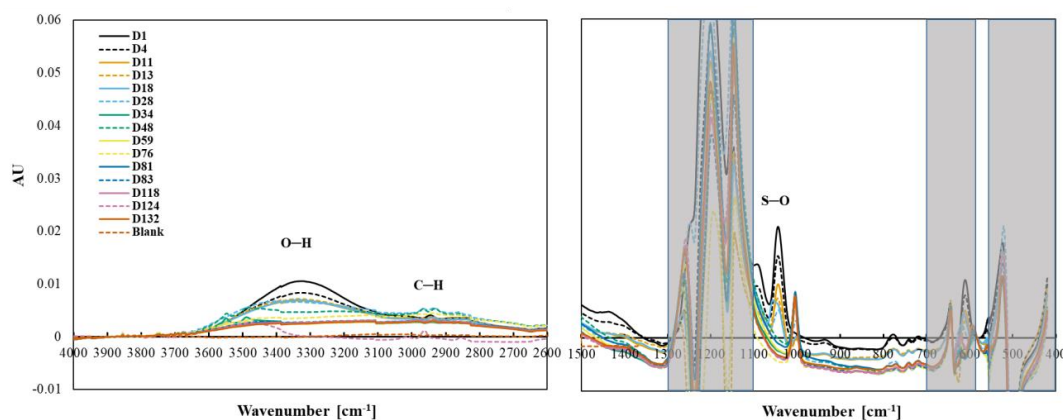
375

376   Figure 4. Changes on the functional group frequency region of hydroxymethanesulfonate (HMS)

377   over 4.1 months.

378

379   Observed peaks at 1094 cm$^{-1}$ and 1041 cm$^{-1}$ are similar to the 1080 cm$^{-1}$ and 1040 cm$^{-1}$ peaks

380   identified as S-O or S=O bonds in FT-IR spectra of Na HMS (Sato et al., 1984) and of HMS

381   (Larkin, 2018; Shurvell, 2006). A weak band at 611 cm$^{-1}$ is like due to C-S (Lin-Vien et al.,

382   1991; Sato et al., 1984) or S-O (Sato et al., 1984) but is obscured by PTFE absorbance. Above

383   1500 cm$^{-1}$ and similar to many aliphatic organic molecules, an O–H (broad peak centered near

384   3300 cm$^{-1}$) and C-H (below 3000 cm$^{-1}$) peaks were observed (Pavia et al., 2008; Shurvell, 2006).

385   Observed peaks are similar to spectral absorbance, although not all peaks in the reference spectra

386   (AIST: SDBS, 2022, See Table S1 in Supplemental Material) are observed in the measured

387   spectra. HMS has a very low vapor pressure (0.00000073 mmHg), (U.S. EPA. Comptox

388   Chemicals Dashboard, 2022) indicating that HMS should not volatilize off the filter.

389   All peaks below 1500 cm$^{-1}$ decrease and are no longer visible by day 34, consistent with the

390   decline but not the extent of decline in mass as the HMS peaks are completely gone and the mass

391   has only decreased by 40%. This behavior is most clearly observed in the peak at 1041 cm$^{-1}$, but

392   also observed in 1094 cm$^{-1}$ peak (Figure 4). Similar to the S-O/S=O peaks, C-H peaks decline

393   during the first 34 days and then completely disappear. The O-H peak, centered around 3300 cm$^{-}$

394   $^{1}$, disappears more slowly, but like the S-O and C-H peaks, is gone by the end of the experiment.

395   Counter balancing the loss of mass, a new peak becomes visible at 1003 cm$^{-1}$ after 11 days and

396   increases for the rest of the study. The peak at 1003 cm$^{-1}$ is tentatively identified as bisulfate

397   (Boer et al., 2007; Krost and McClenny, 1994).  The small peak centered around 3450 cm$^{-1}$

398   becomes evident as the O-H peak disappears and may indicate the presence of condensed water

399   (Boer et al., 2007).

400       IC and ICP-OES
401
402   Sixteen HMS PTFE filters were analyzed by IC with recoveries of 65 ± 4% and calibration

403   verification solution recoveries of 94 ± 5%.  ICP-OES analysis was not performed on these

404   filters.  Eight additional HMS filters (65 µg – 100 µg) were shipped to RTI and 2 filters were

405   extracted and analyzed by IC and ICP-OES on each of the following days 0, 30, 61, and 101.

406   The sulfur mass losses in IC (Figure S3, Supplemental Material) over the 101 days is ~60% loss

407   from the initial weighed mass or about 39% loss assuming a constant extraction efficiency of

408   65% for all samples and is in agreement with the 38% decrease in mass on the filter measured by

409    gravimetry. Similar results were obtained for ICP-OES.  IC analysis (Figure 5) confirms the

410    samples are mostly HMS on day zero but over time the HMS is converted to sulfate (sulfate and

411    bisulfate are indistinguishable in IC), supporting assignment of the 1003 cm$^{-1}$ infrared peak to

412    inorganic bisulfate.  A small amount of the HMS may be converting to sulfate in solution or the

413    column, but the measured changes are much larger than what is expected due to that mechanism

414    alone.  The small amount of HMS that is measured by IC on day 60 and 101 are near detection

415    limits for IC which corroborate the absence of HMS in the FT-IR spectra after two months. The

416    IC and FT-IR results both show a conversion of HMS into sulfate indicating that HMS is not

417    stable and cannot be quantified reliably on PTFE filters in IMPROVE by either FT-IR or IC. In

418    Moch et al. (2020), HMS did not degrade over time under cold storage conditions on nylon

419    filters from IMPROVE suggesting that storage or perhaps filter type may play an important role

420    in HMS degradation on filters.
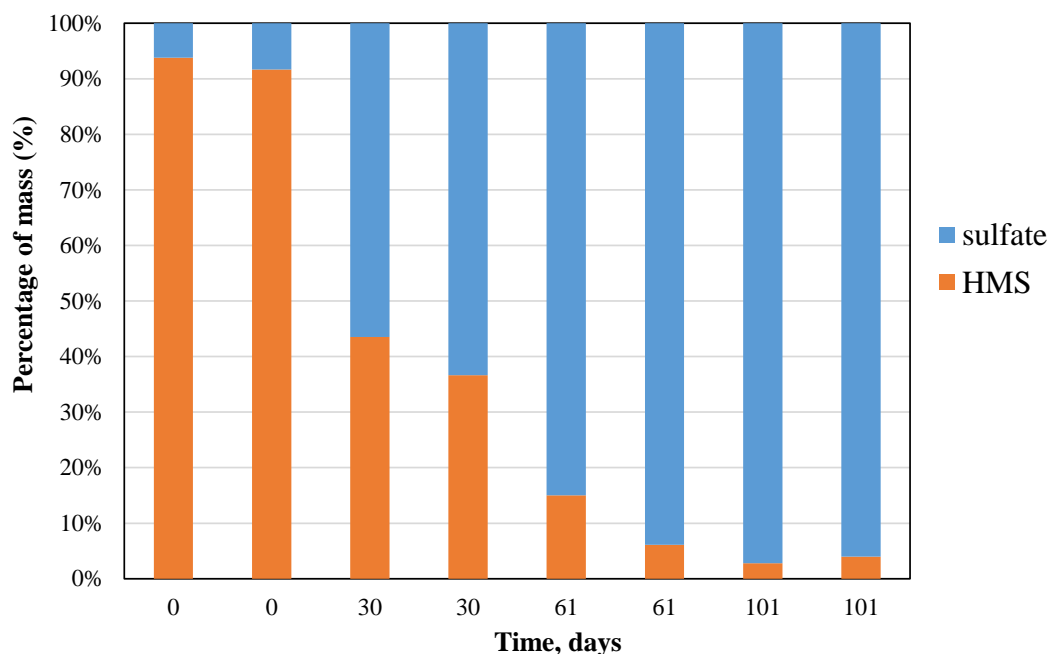
421

422   Figure 5. Percentage of HMS and sulfate measured by IC.  Eight PTFE filters were extracted and

423   analyzed in pairs over 101 days.

**Methyl sulfate**

425       Gravimetry

426   Mass measurements of methyl sulfate salt over a 4 -month period were within measurement

427   uncertainty for the three filters loaded with approximately 30 µg of methyl sulfate (the change

428   over time was indistinguishable from zero). For the 60 µg filters (Figure 6), the first 2 months

429   and the last two weeks mass change were within measurement uncertainty ($\pm$ 6 µg). However,

430   for about a month, between day 70 and 100, much of the data (except day 91) is outside of

431   measurement uncertainty, indicating mass loss of between 10 and 20%. During this period only

432   one spectrum (day 79) was collected, and it does not support mass loss. Day 100 spectra, and all

433   spectra collected through the end of the study, for all three 60 ug loadings, filter samples

434   confirms no changes in the MS compound. Mass and spectral data indicate stability of mostly

435   stable MS on filters under ambient laboratory condition (24°C).
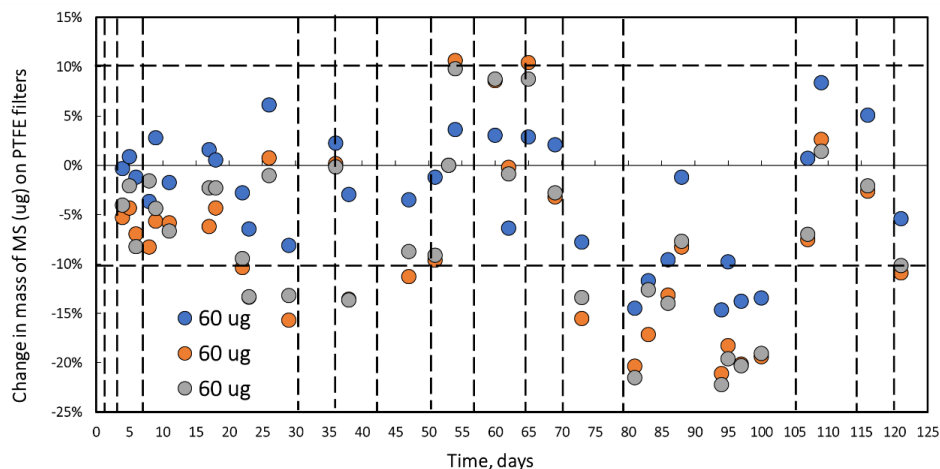
436

437    Figure 6. Mass behavior of methyl sulfate (MS) standard over 4 months. Dotted vertical lines

438    indicate FT-IR analysis. Horizontal broken line indicates mass balance precision for PTFE 25-

439    mm diameter filters.

440        FT-IR

441    Methyl sulfate ($CH_3SO_4H$) is composed of a methyl ($CH_3$) group attached to a sulfate ($SO_4$)

442    group with C-O-S bond.  The chemical used in this study is sodium methyl sulfate ($CH_3SO_4Na$).

443    Methyl sulfate aerosol collected on  PTFE filters has two peaks between 4000 cm$^{-1}$ and 2000 cm$^{-1}$

444    $^1$ and eight peaks between 1500 and 500 cm$^{-1}$ (Figure 7), similar to reference spectra in Table S1

445    (AIST: SDBS, 2022). The doublets observed at 1020 cm$^{-1}$, 1000 cm$^{-1}$ and the nearly overlapping

446    peaks at 795 cm$^{-1}$ and 784 cm$^{-1}$ are identified as S-O-C by both FT-IR  (Chihara, 1958; Lloyd et

447    al., 1961; Lloyd and Dodgson, 1961; Segneanu et al., 2012; Shurvell, 2006) and Raman

448    (Okabayashi et al., 1974). The S─O peaks from sulfate are observed around 1073 cm$^{-1}$ and 591

449    cm$^{-1}$ in the spectra, similar to the previous study where peaks from 591 cm$^{-1}$ to 593 cm$^{-1}$,  and at

450    1063 cm$^{-1}$ (solid) and 1081 cm$^{-1}$ (solution) were ascribed to sulfate in potassium methyl sulfate

451    (Chihara, 1958). There is a weak S=O peak at 1458 cm$^{-1}$ (Segneanu et al., 2012).  The O-H

452    group (assuming the Na ion was replaced by H for some of the molecules) at 3500 cm$^{-1}$ is also

453    fairly weak. All collected spectra for one sample are shown, with the exception of day 91 data,

454    which appeared to be anomalous (Supplemental Material, Figure S4 all spectra including day

455    91).

456    The stability of the spectra over 4 months suggests that MS is stable when collected on a PTFE

457    filter. There were no major or consistent changes in peaks associated with S─O─C, S─O, Na-O

458    and C─H.

459   The pattern of change in the peak height of the 3500 cm$^{-1}$ peak does not correlate with the

460   change in mass. Day 1 and day 30 spectra have smaller O-H peak intensities prior to mass

461   decline, compared to and the O-H peak in the spectrum from day 79, when mass had decreased

462   the mass is low, is higher than both.  No consistent difference in the FT-IR spectra was observed

463   on day 79 (low gravimetric mass day) or the following days (days 105 – 120) suggesting that the

464   mass loss seen in the gravimetric data is erroneous.  The high melting and boiling points of MS

465   are 96 °C and 298 °C, respectively and the low vapor pressure of 0.0038 mmHg (U.S. EPA.

466   Comptox Chemicals Dashboard, 2022) indicating that MS is not volatilizing off the filter.

467
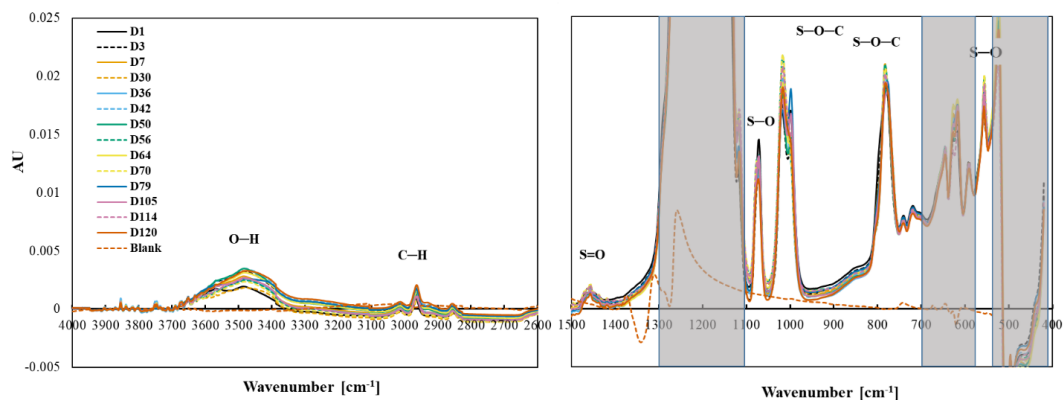
469   Figure 7. Changes in the spectra of MS over a 4- month period. The shaded area indicates the

470   absorbance regions of PTFE filter.

471         IC and ICP-OES

472   Sixteen PTFE samples, eight with mass loadings between 38 µg – 57 µg and eight with higher

473   mass loadings, between 98 µg – 118 µg, were prepared for IC and ICP-OES analysis.  Eight

474   PTFE filters were extracted on day 0 and recoveries were 60 ± 1% for IC and 87 ± 3% for ICP-

475   OES analyses. Recoveries of calibration verification solutions were 100 ± 1% for IC and 97 ±

476   6% for ICP-OES.  Additional filters were extracted on day 39 and 61 showed recoveries

477    consistent with recoveries measured during the initial extracts, $59 \pm 2\%$ for IC and $86 \pm 4\%$ for

478    ICP-OES.  The overall lower mass recovery is indicative that not all MS is extracted from the

479    filter and the lower recoveries by IC compared to ICP-OES, suggests that MS is converting to

480    another sulfur compound in solution.  The consistency in recoveries over time indicates stability

481    of MS on PTFE over this time period, which is in agreement with the mass stability of as shown

482    by gravimetric over the course of the experiment. Unfortunately, filters were not extracted during

483    the time period when the gravimetric results show a small deviation from stability.

484    MS is stable on a PTFE filter as indicated by gravimetry, FT-IR and IC suggesting that at least

485    some atmospherically relevant organosulfates can be measured on PTFE filters in IMPROVE by

486    FT-IR.

487    **2-Methyltetrol sulfate**

488        Gravimetry

489    Mass changes in three 2-methyltetrol sulfate ($C_5H_{11}SO_7$) filter samples with concentrations from

490    55 µg to 57 µg are shown in Figure 8. Mass decreases during the first 23 days to 73% of the

491    initial mass ($25\% \pm 2\%$).  No additional mass loss was observed after 25 days. Mass behavior

492    indicates a loss of 2-MTS on filters under ambient laboratory condition (24°C).  Similar results

493    were obtained for filters weighing approximately 40 µg.

494
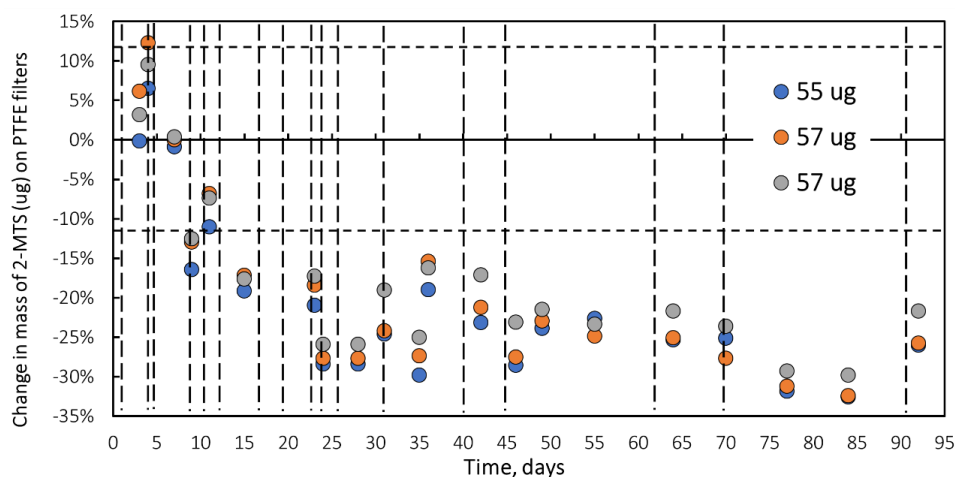
Figure 8. Change in mass of 2-MTS collected on PTFE filters over a 3-month period under

laboratory conditions. Dotted vertical lines indicate FT-IR analysis. Horizontal broken red line

indicates mass balance precision.

FT-IR

2-Methyltetrol sulfate ($C_5H_{11}SO_7$) is a branched compound with 3 units of –OH, one methyl

group and a sulfate group. Like methyl sulfate, 2-methyltetrol sulfate is an organosulfate and has

a C-O-S bond.  2-MTS collected on PTFE filters has broad, organic-related peaks between 4000

$cm^{-1}$ and 2500 $cm^{-1}$ and four peaks between 1500 and 500 $cm^{-1}$ (Figure 9). Observed peaks can

be ascribed to functional groups with the molecule based on previous FT-IR and Raman work

(Bondy et al., 2018; Fankhauser et al., 2022; Lloyd et al., 1961; Lloyd and Dodgson, 1961).

505
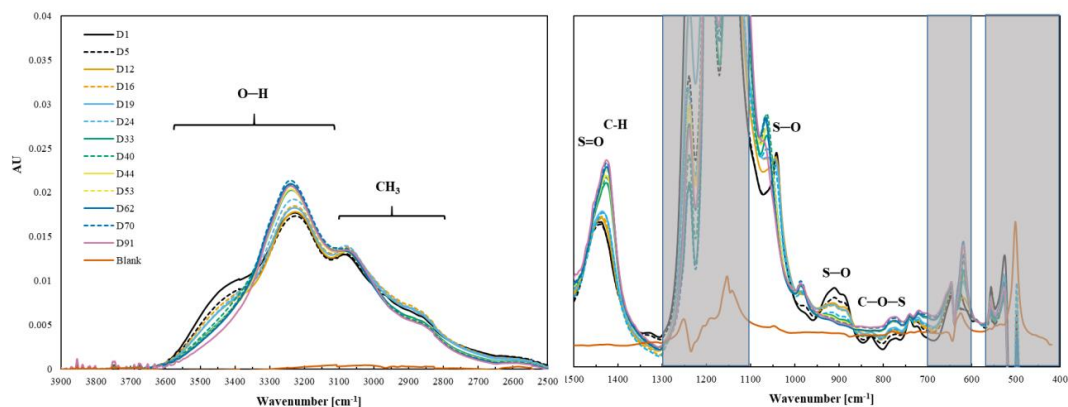
Figure 9. Changes in the spectra of 2-MTS over a 3-month period. The shaded area indicates the

507    absorbance regions of PTFE filter.

508    The observed peak at 1041 cm$^{-1}$ is ascribed to S-O stretch (Bondy et al., 2018; Fankhauser et al.,

509    2022), as it is similar to the peak of MS at 1050 cm$^{-1}$ (Lloyd et al., 1961; Lloyd and Dodgson,

510    1961).  The doublet at 908 cm$^{-1}$ and 898 cm$^{-1}$ correspond to symmetric and asymmetric stretch of

511    S-O of 2-MTS (Fankhauser et al., 2022). The weak peak at 827 cm$^{-1}$ is tentatively assigned to C-

512    O-S stretch based on Raman spectra of 3-MTS (Bondy et al., 2018). The peak at 1446 cm$^{-1}$ is

513    tentatively assigned  to asymmetric S=O stretch based on density functional theory of FT-IR

514    spectra of 2-MTS (Fankhauser et al., 2022) and the assignment of S=O to peak at 1448 cm$^{-1}$ in

515    methyl sulfate (Bondy et al., 2018).  However, this peak was suggested to be due to C-H using

516    density functional theory of Raman spectra of 2-methyltetrol sulfates (Bondy et al., 2018) and

517    commonly ascribed to CH$_2$ in organic molecules at ~1465 cm$^{-1}$ (Pavia et al., 2008).  We decided

518    to assign this to S=O because the sulfate related peaks are strong and the C-H peaks are very

519    weak in this molecule. In the higher frequency region, the very subtle peak at 2879 cm$^{-1}$ is

520    ascribed to C-H stretch and the large broad peaks at 3065 and cm$^{-1}$, 3210 cm$^{-1}$ and shoulder at

521    3426 cm$^{-1}$ may be attributable to –OH stretch (Bondy et al., 2018; Fankhauser et al., 2022;

522    Larkin, 2018; Shurvell, 2006) or inorganic –NH stretch (Boer et al., 2007; Larkin, 2018). Our

523    tentative peaks assignments of ammonium at 3210 cm$^{-1}$ and 3065 cm$^{-1}$ and OH at 3426 cm$^{-1}$ are

524    based on changes in spectra discussed below.

525         Most of 2-MTS infrared peaks decreased and disappeared over time, consistent with the

526    decline in mass.  The S-O peaks at 1041 cm$^{-1}$, 908 cm$^{-1}$ and 898 cm$^{-1}$ decreased and were gone

527    by day 40. The weak C-O-S peak at 827 cm$^{-1}$ disappeared by day 26. The C-H region at 3000-

528    2800 cm$^{-1}$ decreased, similar to the changes in S-O-C peaks. However, some peaks shifted or

529    new peaks formed.  New peaks (or possibly shifts from 1041 cm$^{-1}$ and 908 cm$^{-1}$ doublet) at 1066

530    cm$^{-1}$ and at 987 cm$^{-1}$ appear on day 40 and then increase slightly over time. The S=O peak at

531    1446 cm$^{-1}$ behaves differently from other 2-MTS peaks and  increases slightly until day 33 when

532    the peak height increased significantly and shifted to 1420 cm$^{-1}$ where it continues to grow

533    increase over time. Two peaks at 3210 cm$^{-1}$ and 3065 cm$^{-1}$ increased whereas the region around

534    3450-3550 cm$^{-1}$ decreased, indicating that the shoulder at 3450 cm$^{-1}$ arises from a different bond

535    than the peaks at 3210 cm$^{-1}$ and 3065 cm$^{-1}$.

536    The changes in the spectra indicate a change in the chemical composition on the filter.  2-MTS is

537    no longer present by mid-way through the experiment as evidenced by the disappearance of S-O,

538    C-O-S, C-H and O-H peaks.  This result is supported by a study of ambient 2-MTS that showed

539    that the atmospheric lifetime of 2-MTS is to be about 16 days (Chen et al., 2020). Intermediate

540    oxidation products of 2-MTS transformation include other organosulfates such as 2-

541    methylglyceric acid organosulfate ($C_4H_7SO_7$, MGOS) and glycolic acid organosulfate ($C_2H_3SO_6$,

542    GAS) (Chen et al., 2020; Zhao et al., 2020) and the final product is likely inorganic $(NH_4)_2SO_4$

543    (Harrill, 2020; Zhao et al., 2020).  Raman spectra of MGOS (Bondy et al., 2018) indicate that the

544    spectra at the end of the experiment could be 2-MGOS.  The increased peak at 3210 cm$^{-1}$ and

545    3065 cm$^{-1}$ could be associated with –OH stretch and CH$_3$ asymmetric stretch of 2-MGOS and the

546    1420 cm$^{-1}$ (C-H), 1066 cm$^{-1}$ (S-O) and 987 cm$^{-1}$ (SO4$^{2-}$) match the final spectra well.  The

547    carbonyl group in 2-MGOS is very weak in the Raman spectra and indistinguishable from a

548    blank filter in the final FT-IR spectra in this project.  Alternatively, the final spectra could be

549    ammonium sulfate as indicated by peaks at 3210 cm$^{-1}$, 3065 cm$^{-1}$  and 1420 cm$^{-1}$  which are

550    indicative of ammonium, however, the 1066 cm$^{-1}$ and 987 cm$^{-1}$ peaks are lower than typically

551    observed for inorganic ammonium sulfate (Boer et al., 2007; Zawadowicz et al., 2015)

552    suggesting this is not inorganic sulfate. There are limited FT-IR or Raman spectra of the many

553    oxidation products of 2-MTS so definitive identification is not possible and it is likely that there

554    is a mixture of oxidation products present on the filter.

555    To further evaluate the possible compounds on the filter at the end of the experiment, mass loss

556    calculations were performed.  If 2-MTS is converted completely to MGOS, the mass loss would

557    be only 7%.  If 2-MTS is converted completely to GAS, the mass loss would be 28% and if 2-

558    MTS is converted completely to ammonium sulfate the mass loss would be 39%.  These values

559    span the observed mass loss at 25% which suggesting that the compounds on the filter are of an

560    intermediate type and still in the organosulfate form not inorganic ammonium sulfate.

561        IC and ICP-OES

562    Sixteen PTFE samples, eight with mass loading between 11– 28 μg and eight with higher mass

563    loadings, between 37 – 46 μg were extracted immediately upon receipt at RTI. The IC showed

564    low sensitivity to 2-MTS detection and results are not reported so no additional information was

565    available about what compounds the 2-MTS may have change into.  Given that ICP-OES

566    measures sulfur and not individual compounds, the results from this method do not provide

567     insight into chemical conversions on the filter but are briefly discussed in the supplemental

568     material (Figure S5).

# 4. Conclusions

570     The stability and therefore potential for FT-IR to measure organosulfur and

571     organosulfates collected on PTFE filters varies by compound. MS has the highest potential to be

572     measured on PTFE filters in IMPROVE samples by FT-IR, due to its minimal mass change and

573     no spectral changes. Consistent recoveries by IC and ICP-OES over multiple months of analysis

574     support the conclusion that MS is stable on the filters.  Consistent results from analysis at UC

575     Davis and RTI suggest robustness to storage, shipping and handling conditions.  MS is one of

576     many organosulfates observed in the atmosphere and not necessarily representative of

577     organosulates in general as indicated by 2-MTS.  Gravimetric mass suggests some (30%) mass

578     loss from 2-MTS samples on the PTFE filter, over a three-month period. FT-IR suggests that 2-

579     MTS is unstable on PTFE filter and changing into different compound(s), likely still an

580     organosulfate.  FT-IR and gravimetry show that MSA can be measured from PTFE filters but

581     due to volatility off the filters a lower bound of MSA is measured (i.e., less than the amount of

582     MSA in the atmosphere). IC further confirmed that MSA did not chemically change while on the

583     filter.  Infrared peaks in HMS spectra mid-way through the experiment indicate that HMS is not

584     stable on PTFE filters and likely converts to bisulfate. IC indicates that HMS is changing to

585     (bi)sulfate over time.  Further investigations of measurements by FT-IR on PTFE of other

586     organosulfates are warranted to evaluate the extent to which the organosulfate functional group

587     can be quantified from IMPROVE PTFE filters. Further work to determine the stability and

588     ability to measure these compounds in aerosol mixtures as found in ambient samples is needed

589     before confidently using FT-IR on IMPROVE samples to measure organic sulfur compounds.

590

591 Author Contribution: Conceptualization: AMD, TD; Formal Analysis: MBA, TD, ST, AMD;

592 Funding: AMD, TD; Investigation: MBA, MDeB, LH, KL; Project Administration: AMD;

593 Supervision: AMD, TD; Writing First Draft: MBA, TD; Writing Revisions and Editing: MBA,

594 ST, TD, MDeB, LH, KL AMD; software: ST, MA; Visualization: MA

595

596 Competing Interests: The contact author has declared that none of the authors has any competing

597 interests.

598

599 Acknowledgements: AMD and MA wish to acknowledge funding from Research Triangle

600 Institute (Agreement No. 62997) and the Interagency Monitoring of Protected Visual

601 Environments (Grant No. P21AC11294). The authors would like to acknowledge Jason Surratt

602 and his team for providing the 2-MTS compound used in this study.

603

604

# 5. References

606 AIST: SDBS, 2022. Spectral Database for Organic Compounds,SDBS [WWW Document]. Spectral
607     Database for Organic Compounds,SDBS. URL https://sdbs.db.aist.go.jp/sdbs/cgi-
608     bin/direct_frame_top.cgi (accessed 2.22.22).
609 Allen, A.G., Davison, B.M., James, J.D., Robertson, L., Harrison, R.M., Hewitt, C.N., 2002. Influence of
610     Transport over a Mountain Ridge on the Chemical Composition of Marine Aerosols during the
611     ACE-2 Hillcloud Experiment. Journal of Atmospheric Chemistry 41, 83–107.
612     https://doi.org/10.1023/A:1013868729960
613 Allen, A.G., Dick, A.L., Davison, B.M., 1997. Sources of atmospheric methanesulphonate, non-sea-salt
614     sulphate, nitrate and related species over the temperate South Pacific. Atmospheric Environment
615     31, 191–205. https://doi.org/10.1016/1352-2310(96)00194-X
616 Amore, A., Giardi, F., Becagli, S., Caiazzo, L., Mazzola, M., Severi, M., Traversi, R., 2022. Source
617     apportionment of sulphate in the High Arctic by a 10 yr-long record from Gruvebadet
618     Observatory (Ny-Ålesund, Svalbard Islands). Atmospheric Environment 270, 118890.
619     https://doi.org/10.1016/j.atmosenv.2021.118890
620 Aneja, V.P., Cooper, W.J., 1989. Biogenic Sulfur Emissions, in: Biogenic Sulfur in the Environment,
621     ACS Symposium Series. American Chemical Society, pp. 2–13. https://doi.org/10.1021/bk-1989-
622     0393.ch001
623 Barnes, I., Becker, K.H., Mihalopoulos, N., 1994. An FTIR product study of the photooxidation of
624     dimethyl disulfide. J Atmos Chem 18, 267–289. https://doi.org/10.1007/BF00696783
625 Bates, T.S., Lamb, B.K., Guenther, A., Dignon, J., Stoiber, R.E., 1992. Sulfur emissions to the
626     atmosphere from natural sourees. J Atmos Chem 14, 315–337.
627     https://doi.org/10.1007/BF00115242
628 Becagli, S., Lazzara, L., Fani, F., Marchese, C., Traversi, R., Severi, M., di Sarra, A., Sferlazzo, D.,
629     Piacentino, S., Bommarito, C., Dayan, U., Udisti, R., 2013. Relationship between
630     methanesulfonate (MS−) in atmospheric particulate and remotely sensed phytoplankton activity
631     in oligo-mesotrophic central Mediterranean Sea. Atmospheric Environment 79, 681–688.
632     https://doi.org/10.1016/j.atmosenv.2013.07.032
633 Boer, G.J., Sokolik, I.N., Martin, S.T., 2007. Infrared optical constants of aqueous sulfate–nitrate–
634     ammonium multi-component tropospheric aerosols from attenuated total reflectance
635     measurements—Part I: Results and analysis of spectral absorbing features. Journal of
636     Quantitative Spectroscopy and Radiative Transfer 108, 17–38.
637     https://doi.org/10.1016/j.jqsrt.2007.02.017
638 Bondy, A.L., Craig, R.L., Zhang, Z., Gold, A., Surratt, J.D., Ault, A.P., 2018. Isoprene-Derived
639     Organosulfates: Vibrational Mode Analysis by Raman Spectroscopy, Acidity-Dependent Spectral
640     Modes, and Observation in Individual Atmospheric Particles. J. Phys. Chem. A 122, 303–315.
641     https://doi.org/10.1021/acs.jpca.7b10587
642 Boris, A.J., Takahama, S., Weakley, A.T., Debus, B.M., Fredrickson, C.D., Esparza-Sanchez, M., Burki,
643     C., Reggente, M., Shaw, S.L., Edgerton, E.S., Dillner, A.M., 2019. Quantifying organic matter
644     and functional groups in particulate matter filter samples from the southeastern United States –
645     Part 1: Methods. Atmospheric Measurement Techniques 12, 5391–5415.
646     https://doi.org/10.5194/amt-12-5391-2019
647 Boris, A.J., Takahama, S., Weakley, A.T., Debus, B.M., Shaw, S.L., Edgerton, E.S., Joo, T., Ng, N.L.,
648     Dillner, A.M., 2021. Quantifying organic matter and functional groups in particulate matter filter
649     samples from the southeastern United States – Part 2: Spatiotemporal trends. Atmospheric
650     Measurement Techniques 14, 4355–4374. https://doi.org/10.5194/amt-14-4355-2021
651 Campbell, J.R., Battaglia, M.Jr., Dingilian, K., Cesler-Maloney, M., St Clair, J.M., Hanisco, T.F.,
652     Robinson, E., DeCarlo, P., Simpson, W., Nenes, A., Weber, R.J., Mao, J., 2022. Source and

653        Chemistry of Hydroxymethanesulfonate (HMS) in Fairbanks, Alaska. Environ. Sci. Technol. 56,
654        7657–7667. https://doi.org/10.1021/acs.est.2c00410
655 Chackalackal, S.M., Stafford, F.E., 1966. Infrared Spectra of Methane-, Fluoro-, and Chlorosulfonic
656        Acids. J. Am. Chem. Soc. 88, 4815–4819. https://doi.org/10.1021/ja00973a010
657 Chapman, E.G., Barinaga, C.J., Udseth, H.R., Smith, R.D., 1990. Confirmation and quantitation of
658        hydroxymethanesulfonate in precipitation by electrospray ionization-tandem mass spectrometry.
659        Atmospheric Environment. Part A. General Topics 24, 2951–2957. https://doi.org/10.1016/0960-
660        1686(90)90475-3
661 Chen, C., Zhang, Z., Wei, L., Qiu, Y., Xu, Weiqi, Song, S., Sun, J., Li, Z., Chen, Y., Ma, N., Xu,
662        Wanyun, Pan, X., Fu, P., Sun, Y., 2022. The importance of hydroxymethanesulfonate (HMS) in
663        winter haze episodes in North China Plain. Environmental Research 211, 113093.
664        https://doi.org/10.1016/j.envres.2022.113093
665 Chen, Y., Dombek, T., Hand, J., Zhang, Z., Gold, A., Ault, A.P., Levine, K.E., Surratt, J.D., 2021.
666        Seasonal Contribution of Isoprene-Derived Organosulfates to Total Water-Soluble Fine
667        Particulate Organic Sulfur in the United States. ACS Earth Space Chem. 5, 2419–2432.
668        https://doi.org/10.1021/acsearthspacechem.1c00102
669 Chen, Y., Zhang, Y., Lambe, A.T., Xu, R., Lei, Z., Olson, N.E., Zhang, Z., Szalkowski, T., Cui, T.,
670        Vizuete, W., Gold, A., Turpin, B.J., Ault, A.P., Chan, M.N., Surratt, J.D., 2020. Heterogeneous
671        Hydroxyl Radical Oxidation of Isoprene-Epoxydiol-Derived Methyltetrol Sulfates: Plausible
672        Formation Mechanisms of Previously Unexplained Organosulfates in Ambient Fine Aerosols.
673        Environ. Sci. Technol. Lett. 7, 460–468. https://doi.org/10.1021/acs.estlett.0c00276
674 Chihara, G., 1958. Measurement of Infrared Absorption Spectra by Absorption on Japanese Hand-made
675        Paper and Its Application to Paper Chromatography. Chemical & Pharmaceutical Bulletin 6, 143–
676        147. https://doi.org/10.1248/cpb.6.143
677 Debus, B., Takahama, S., Weakley, A.T., Seibert, K., Dillner, A.M., 2019. Long-Term Strategy for
678        Assessing Carbonaceous Particulate Matter Concentrations from Multiple Fourier Transform
679        Infrared (FT-IR) Instruments: Influence of Spectral Dissimilarities on Multivariate Calibration
680        Performance. Appl Spectrosc 73, 271–283. https://doi.org/10.1177/0003702818804574
681 Debus, B., Weakley, A.T., Takahama, S., George, K.M., Amiri-Farahani, A., Schichtel, B., Copeland, S.,
682        Wexler, A.S., Dillner, A.M., 2022. Quantification of major particulate matter species from a
683        single filter type using infrared spectroscopy – application to a large-scale monitoring network.
684        Atmospheric Measurement Techniques 15, 2685–2702. https://doi.org/10.5194/amt-15-2685-
685        2022
686 Decesari, S., Facchini, M.C., Fuzzi, S., Tagliavini, E., 2000. Characterization of water-soluble organic
687        compounds in atmospheric aerosol: A new approach. Journal of Geophysical Research:
688        Atmospheres 105, 1481–1489. https://doi.org/10.1029/1999JD900950
689 Dovrou, E., Lim, C.Y., Canagaratna, M.R., Kroll, J.H., Worsnop, D.R., Keutsch, F.N., 2019.
690        Measurement techniques for identifying and quantifying hydroxymethanesulfonate (HMS) in an
691        aqueous matrix and particulate matter using aerosol mass spectrometry and ion chromatography.
692        Atmospheric Measurement Techniques 12, 5303–5315. https://doi.org/10.5194/amt-12-5303-
693        2019
694 Fankhauser, A.M., Lei, Z., Daley, K.R., Xiao, Y., Zhang, Z., Gold, A., Ault, B.S., Surratt, J.D., Ault,
695        A.P., 2022. Acidity-Dependent Atmospheric Organosulfate Structures and Spectra: Exploration
696        of Protonation State Effects via Raman and Infrared Spectroscopies Combined with Density
697        Functional Theory. J. Phys. Chem. A 126, 5974–5984. https://doi.org/10.1021/acs.jpca.2c04548
698 Frossard, A.A., Shaw, P.M., Russell, L.M., Kroll, J.H., Canagaratna, M.R., Worsnop, D.R., Quinn, P.K.,
699        Bates, T.S., 2011. Springtime Arctic haze contributions of submicron organic particles from
700        European and Asian combustion sources. Journal of Geophysical Research: Atmospheres 116.
701        https://doi.org/10.1029/2010JD015178
702 Grübler, A., 1998. A Review of Global and Regional Sulfur Emission Scenarios. Mitigation and
703        Adaptation Strategies for Global Change 3, 383–418. https://doi.org/10.1023/A:1009651624257

704  Hansen, A.M.K., Kristensen, K., Nguyen, Q.T., Zare, A., Cozzi, F., Nøjgaard, J.K., Skov, H., Brandt, J.,
705      Christensen, J.H., Ström, J., Tunved, P., Krejci, R., Glasius, M., 2014. Organosulfates and
706      organic acids in Arctic aerosols: speciation, annual variation and concentration levels.
707      Atmospheric Chemistry & Physics 14, 7807–7823. https://doi.org/10.5194/acp-14-7807-2014
708  Harrill, A.J., 2020. Aqueous-Phase Processing of 2-Methyltetrol Sulfates by Hydroxyl Radical Oxidation
709      in Fog and Cloud Water Mimics: Implications for Isoprene-Derived Secondary Organic Aerosol.
710  Hawkins, L.N., Russell, L.M., Covert, D.S., Quinn, P.K., Bates, T.S., 2010. Carboxylic acids, sulfates,
711      and organosulfates in processed continental organic aerosol over the southeast Pacific Ocean
712      during VOCALS-REx 2008. Journal of Geophysical Research: Atmospheres 115.
713      https://doi.org/10.1029/2009JD013276
714  Hettiyadura, A.P.S., Jayarathne, T., Baumann, K., Goldstein, A.H., de Gouw, J.A., Koss, A., Keutsch,
715      F.N., Skog, K., Stone, E.A., 2017. Qualitative and quantitative analysis of atmospheric
716      organosulfates in Centreville, Alabama. Atmospheric Chemistry and Physics 17, 1343–1359.
717      https://doi.org/10.5194/acp-17-1343-2017
718  Hettiyadura, A.P.S., Stone, E.A., Kundu, S., Baker, Z., Geddes, E., Richards, K., Humphry, T., 2015.
719      Determination of atmospheric organosulfates using HILIC chromatography with MS detection.
720      Atmospheric Measurement Techniques 8, 2347–2358. https://doi.org/10.5194/amt-8-2347-2015
721  Hoffmann, E.H., Tilgner, A., Schrödner, R., Bräuer, P., Wolke, R., Herrmann, H., 2016. An advanced
722      modeling study on the impacts and atmospheric implications of multiphase dimethyl sulfide
723      chemistry. PNAS 113, 11776–11781.
724  Kamruzzaman, M., Takahama, S., Dillner, A.M., 2018. Quantification of amine functional groups and
725      their influence on OM/OC in the IMPROVE network. Atmospheric Environment 172, 124–132.
726      https://doi.org/10.1016/j.atmosenv.2017.10.053
727  Knovel, C.L., 2014. Knovel - Yaws' Critical Property Data for Chemical Engineers and Chemists - Table
728      12. Vapor Pressure - Organic Compounds, log P = A - B/(T + C) [WWW Document]. URL
729      https://app.knovel.com/kn/resources/kt009ZN2S3/kpYCPDCECD/eptble/itable?b-
730      =&columns=1%2C2%2C3%2C6%2C4%2C5%2C10%2C11%2C13%2C14%2C12%2C7%2C8%
731      2C9 (accessed 9.7.22).
732  Krost, K.J., McClenny, W.A., 1994. FT-IR Transmission Spectroscopy for Quantitation of Ammonium
733      Bisulfate in Fine-Particulate Matter Collected on Teflon® Filters. Appl. Spectrosc., AS 48, 702–
734      705.
735  Kuzmiakova, A., Dillner, A.M., Takahama, S., 2016. An automated baseline correction protocol for
736      infrared spectra of atmospheric aerosols collected on polytetrafluoroethylene (Teflon) filters.
737      Atmospheric Measurement Techniques 9, 2615–2631. https://doi.org/10.5194/amt-9-2615-2016
738  Kwong, K.C., Chim, M.M., Davies, J.F., Wilson, K.R., Chan, M.N., 2018a. Importance of sulfate radical
739      anion formation and chemistry in heterogeneous OH oxidation of sodium methyl sulfate, the
740      smallest organosulfate. Atmos. Chem. Phys. 18, 2809–2820. https://doi.org/10.5194/acp-18-
741      2809-2018
742  Kwong, K.C., Chim, M.M., Hoffmann, E.H., Tilgner, A., Herrmann, H., Davies, J.F., Wilson, K.R.,
743      Chan, M.N., 2018b. Chemical Transformation of Methanesulfonic Acid and Sodium
744      Methanesulfonate through Heterogeneous OH Oxidation. ACS Earth Space Chem. 2, 895–903.
745      https://doi.org/10.1021/acsearthspacechem.8b00072
746  Larkin, P.J., 2018. Chapter 6 - IR and Raman Spectra–Structure Correlations: Characteristic Group
747      Frequencies, in: Larkin, P.J. (Ed.), Infrared and Raman Spectroscopy (Second Edition). Elsevier,
748      pp. 85–134. https://doi.org/10.1016/B978-0-12-804162-8.00006-9
749  Laurent, J.-P., Allen, D.T., 2004. Size Distributions of Organic Functional Groups in Ambient Aerosol
750      Collected in Houston, Texas Special Issue of *Aerosol Science and Technology* on Findings from
751      the Fine Particulate Matter Supersites Program. Aerosol Science and Technology 38, 82–91.
752      https://doi.org/10.1080/02786820390229561

753 Lee, J.-K., Lee, J.-S., Ahn, Y.-S., Kang, G.-H., 2019. Restoring the Reactivity of Organic Acid Solution
754     Used for Silver Recovery from Solar Cells by Fractional Distillation. Sustainability 11, 3659.
755     https://doi.org/10.3390/su11133659
756 Lee, S.-H., Murphy, D.M., Thomson, D.S., Middlebrook, A.M., 2003. Nitrate and oxidized organic ions
757     in single particle mass spectra during the 1999 Atlanta Supersite Project. Journal of Geophysical
758     Research: Atmospheres 108, SOS 5-1-SOS 5-8. https://doi.org/10.1029/2001JD001455
759 Lin-Vien, D., Colthup, N.B., Fateley, W.G., Grasselli, J.G., 1991. CHAPTER 14 - Organic Sulfur
760     Compounds, in: Lin-Vien, D., Colthup, N.B., Fateley, W.G., Grasselli, J.G. (Eds.), The
761     Handbook of Infrared and Raman Characteristic Frequencies of Organic Molecules. Academic
762     Press, San Diego, pp. 225–250. https://doi.org/10.1016/B978-0-08-057116-4.50020-1
763 Liu, S., Ahlm, L., Day, D.A., Russell, L.M., Zhao, Y., Gentner, D.R., Weber, R.J., Goldstein, A.H., Jaoui,
764     M., Offenberg, J.H., Kleindienst, T.E., Rubitschun, C., Surratt, J.D., Sheesley, R.J., Scheller, S.,
765     2012. Secondary organic aerosol formation from fossil fuel sources contribute majority of
766     summertime organic mass at Bakersfield: SOA AT BAKERSFIELD. J. Geophys. Res. 117, n/a-
767     n/a. https://doi.org/10.1029/2012JD018170
768 Liu, S., Takahama, S., Russell, L.M., Gilardoni, S., Baumgardner, D., 2009. Oxygenated organic
769     functional groups and their sources in single and submicron organic particles in MILAGRO 2006
770     campaign. Atmospheric Chemistry & Physics 9, 6849–6863. https://doi.org/10.5194/acp-9-6849-
771     2009
772 Lloyd, A.G., Dodgson, K.S., 1961. Infrared studies on sulphate esters. II. Monosaccharide sulphates.
773     Biochim Biophys Acta 46, 116–120. https://doi.org/10.1016/0006-3002(61)90653-9
774 Lloyd, A.G., Dodgson, K.S., Price, R.G., Rose, F.A., 1961. Infrared studies on sulphate esters. I.
775     Polysaccharide sulphates. Biochim Biophys Acta 46, 108–115. https://doi.org/10.1016/0006-
776     3002(61)90652-7
777 Ma, T., Furutani, H., Duan, F., Kimoto, T., Jiang, J., Zhang, Q., Xu, X., Wang, Y., Gao, J., Geng, G., Li,
778     M., Song, S., Ma, Y., Che, F., Wang, J., Zhu, L., Huang, T., Toyoda, M., He, K., 2020.
779     Contribution of hydroxymethanesulfonate (HMS) to severe winter haze in the North China Plain.
780     Atmospheric Chemistry and Physics 20, 5887–5897. https://doi.org/10.5194/acp-20-5887-2020
781 Moch, J.M., Dovrou, E., Mickley, L.J., Keutsch, F.N., Cheng, Y., Jacob, D.J., Jiang, J., Li, M., Munger,
782     J.W., Qiao, X., Zhang, Q., 2018. Contribution of Hydroxymethane Sulfonate to Ambient
783     Particulate Matter: A Potential Explanation for High Particulate Sulfur During Severe Winter
784     Haze in Beijing. Geophysical Research Letters 45, 11,969-11,979.
785     https://doi.org/10.1029/2018GL079309
786 Moch, J.M., Dovrou, E., Mickley, L.J., Keutsch, F.N., Liu, Z., Wang, Y., Dombek, T.L., Kuwata, M.,
787     Budisulistiorini, S.H., Yang, L., Decesari, S., Paglione, M., Alexander, B., Shao, J., Munger,
788     J.W., Jacob, D.J., 2020. Global Importance of Hydroxymethanesulfonate in Ambient Particulate
789     Matter: Implications for Air Quality. Journal of Geophysical Research: Atmospheres 125,
790     e2020JD032706. https://doi.org/10.1029/2020JD032706
791 Okabayashi, H., Okuyama, M., Kitagawa, T., Miyazawa, T., 1974. The Raman Spectra and Molecular
792     Conformations of Surfactants in Aqueous Solution and Crystalline States. BCSJ 47, 1075–1077.
793     https://doi.org/10.1246/bcsj.47.1075
794 Olson, C.N., Galloway, M.M., Yu, G., Hedman, C.J., Lockett, M.R., Yoon, T., Stone, E.A., Smith, L.M.,
795     Keutsch, F.N., 2011. Hydroxycarboxylic Acid-Derived Organosulfates: Synthesis, Stability, and
796     Quantification in Ambient Aerosol. Environ. Sci. Technol. 45, 6468–6474.
797     https://doi.org/10.1021/es201039p
798 Pavia, D.L., Lampman, G.M., Kriz, G.S., Vyvyan, J.A., 2008. Introduction to Spectroscopy. Cengage
799     Learning.
800 Peng, C., Chan, C.K., 2001. The water cycles of water-soluble organic salts of atmospheric importance.
801     Atmospheric Environment 35, 1183–1192. https://doi.org/10.1016/S1352-2310(00)00426-X

802  Reggente, M., Höhn, R., Takahama, S., 2019. An open platform for Aerosol InfraRed Spectroscopy
803      analysis – AIRSpec. Atmospheric Measurement Techniques 12, 2313–2329.
804      https://doi.org/10.5194/amt-12-2313-2019
805  Russell, L.M., Bahadur, R., Ziemann, P.J., 2011. Identifying organic aerosol sources by comparing
806      functional group composition in chamber and atmospheric particles. Proc. Natl. Acad. Sci. U.S.A.
807      108, 3516–3521. https://doi.org/10.1073/pnas.1006461108
808  Ruthenburg, T.C., Perlin, P.C., Liu, V., McDade, C.E., Dillner, A.M., 2014. Determination of organic
809      matter and organic matter to organic carbon ratios by infrared spectroscopy with application to
810      selected sites in the IMPROVE network. Atmospheric Environment 86, 47–57.
811      https://doi.org/10.1016/j.atmosenv.2013.12.034
812  Saltzman, E.S., Savoie, D.L., Prospero, J.M., Zika, R.G., 1986. Methanesulfonic acid and non-sea-salt
813      sulfate in pacific air: Regional and seasonal variations. J Atmos Chem 4, 227–240.
814      https://doi.org/10.1007/BF00052002
815  Sato, S., Higuchi, S., Tanaka, S., 1984. Structural Examinations of "Sodium FormaldehydeSulfoxylate"
816      by Infrared and Raman Spectroscopy. Nippon Kagaku Kaishi 1984, 1151–1157.
817      https://doi.org/10.1246/nikkashi.1984.1151
818  Segneanu, A.E., Gozescu, I., Dabici, A., Sfirloaga, P., Szabadai, Z., 2012. Organic Compounds FT-IR
819      Spectroscopy, Macro To Nano Spectroscopy. IntechOpen. https://doi.org/10.5772/50183
820  Seinfeld, J.H., Pandis, S.N., 2016. Atmospheric Chemistry and Physics: From Air Pollution to Climate
821      Change. Wiley.
822  Shurvell, H.F., 2006. Spectra– Structure Correlations in the Mid- and Far-Infrared, in: Handbook of
823      Vibrational Spectroscopy. American Cancer Society. https://doi.org/10.1002/0470027320.s4101
824  Smith, S.J., van Aardenne, J., Klimont, Z., Andres, R.J., Volke, A., Delgado Arias, S., 2011.
825      Anthropogenic sulfur dioxide emissions: 1850–2005. Atmospheric Chemistry and Physics 11,
826      1101–1116. https://doi.org/10.5194/acp-11-1101-2011
827  Song, S., Gao, M., Xu, W., Sun, Y., Worsnop, D.R., Jayne, J.T., Zhang, Y., Zhu, L., Li, M., Zhou, Z.,
828      Cheng, C., Lv, Y., Wang, Ying, Peng, W., Xu, X., Lin, N., Wang, Yuxuan, Wang, S., Munger,
829      J.W., Jacob, D.J., McElroy, M.B., 2019. Possible heterogeneous chemistry of
830      hydroxymethanesulfonate (HMS) in northern China winter haze. Atmospheric Chemistry and
831      Physics 19, 1357–1371. https://doi.org/10.5194/acp-19-1357-2019
832  Stone, E.A., Yang, L., Yu, L.E., Rupakheti, M., 2012. Characterization of organosulfates in atmospheric
833      aerosols at Four Asian locations. Atmospheric Environment 47, 323–329.
834      https://doi.org/10.1016/j.atmosenv.2011.10.058
835  Surratt, J.D., Chan, A.W.H., Eddingsaas, N.C., Chan, M., Loza, C.L., Kwan, A.J., Hersey, S.P., Flagan,
836      R.C., Wennberg, P.O., Seinfeld, J.H., 2010. Reactive intermediates revealed in secondary organic
837      aerosol formation from isoprene. Proceedings of the National Academy of Sciences 107, 6640–
838      6645. https://doi.org/10.1073/pnas.0911114107
839  Tang, K., 2020. Chemical Diversity and Biochemical Transformation of Biogenic Organic Sulfur in the
840      Ocean. Frontiers in Marine Science 7.
841  U.S. EPA. Comptox Chemicals Dashboard, 2022.
842      https://comptox.epa.gov/dashboard/chemical/details/DTXSID80805075 (accessed November 14,
843      2022) Methyl 10,10-diethoxydec-2-ene-4,6,8-triynoate.
844  von Glasow, R., Crutzen, P.J., 2004. Model study of multiphase DMS oxidation with a focus on halogens.
845      Atmospheric Chemistry and Physics 4, 589–608. https://doi.org/10.5194/acp-4-589-2004
846  Wang, Yao, Zhao, Y., Wang, Yuchen, Yu, J.-Z., Shao, J., Liu, P., Zhu, W., Cheng, Z., Li, Z., Yan, N.,
847      Xiao, H., 2021. Organosulfates in atmospheric aerosols in Shanghai, China: seasonal and
848      interannual variability, origin, and formation mechanisms. Atmospheric Chemistry and Physics
849      21, 2959–2980. https://doi.org/10.5194/acp-21-2959-2021
850  Wei, L., Fu, P., Chen, X., An, N., Yue, S., Ren, H., Zhao, W., Xie, Q., Sun, Y., Zhu, Q.-F., Wang, Z.,
851      Feng, Y.-Q., 2020. Quantitative Determination of Hydroxymethanesulfonate (HMS) Using Ion
852      Chromatography and UHPLC-LTQ-Orbitrap Mass Spectrometry: A Missing Source of Sulfur

853        during Haze Episodes in Beijing. Environ. Sci. Technol. Lett. 7, 701–707.
854        https://doi.org/10.1021/acs.estlett.0c00528
855   Yazdani, A., Dudani, N., Takahama, S., Bertrand, A., Prévôt, A.S.H., El Haddad, I., Dillner, A.M., 2022.
856        Fragment ion–functional group relationships in organic aerosols using aerosol mass spectrometry
857        and mid-infrared spectroscopy. Atmospheric Measurement Techniques 15, 2857–2874.
858        https://doi.org/10.5194/amt-15-2857-2022
859   Zawadowicz, M.A., Proud, S.R., Seppalainen, S.S., Cziczo, D.J., 2015. Hygroscopic and phase separation
860        properties of ammonium sulfate/organics/water ternary solutions. Atmospheric Chemistry and
861        Physics 15, 8975–8986. https://doi.org/10.5194/acp-15-8975-2015
862   Zeng, G., Kelley, J., Kish, J.D., Liu, Y., 2014. Temperature-Dependent Deliquescent and Efflorescent
863        Properties of Methanesulfonate Sodium Studied by ATR-FTIR Spectroscopy. J. Phys. Chem. A
864        118, 583–591. https://doi.org/10.1021/jp405896y
865   Zhao, X., Shi, X., Ma, X., Zuo, C., Wang, H., Xu, F., Sun, Y., Zhang, Q., 2020. 2-Methyltetrol sulfate
866        ester-initiated nucleation mechanism enhanced by common nucleation precursors: A theory
867        study. Science of The Total Environment 723, 137987.
868        https://doi.org/10.1016/j.scitotenv.2020.137987
869   Zhong, L., Parker, S.F., 2018. Structure and vibrational spectroscopy of methanesulfonic acid. R Soc
870        Open Sci 5, 181363. https://doi.org/10.1098/rsos.181363
871